Jurnal Teknologi

APPLICATION OF TAGUCHI METHOD TO OPTIMIZE ULTRASONIC VIBRATION ASSISTED FUSED DEPOSITION MODELING PROCESS PARAMETERS FOR SURFACE ROUGHNESS

Shajahan Maidin, Azlan Abdullah, Norilani Md. Nor Hayati, Haroun Albaluooshi, Rizal Alkahari

Universiti Teknikal Malaysia Melaka, Hang Tuah Jaya, 76100 Durian Tunggal, Melaka, Malaysia

Graphical Abstract
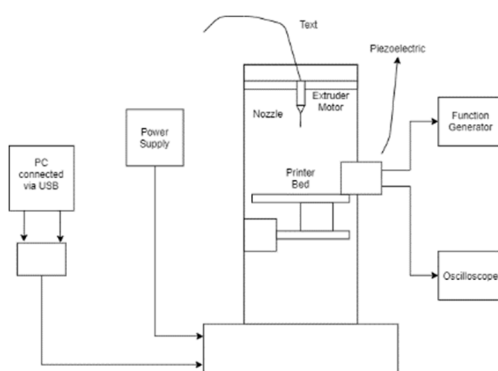
Abstract

This paper presents the findings on the process parameters for surface roughness optimization of an open-source ultrasonic vibration assisted fused deposition modeling (FDM) printed specimen. Acrylonitrile Butadiene Styrene (ABS) material for the specimens and the printing temperature, layer thickness, and surface layer were determined as the control parameters that influenced the surface roughness. Experimental design with Taguchi level 9 (3*3) Orthogonal Arrays (OA) was designed with nine experimental runs. Three levels of each control factor was identified. In addition, data for multi-responses of build time and surface roughness was obtained by utilizing and conducting the nine-requirement experimental run for Taguchi Method. The specimens were printed using an open-source ultrasonic vibration assisted FDM printer with a 20kHz ultrasonic vibration supplied to the printing platform of the printer. Analysis of variance (ANOVA) was conducted to determine whether p-values are significant with the model or otherwise. The experiments examined the build time and surface roughness, the responses were collected and optimized by using the grey relational grade (GRG). The result shows no correlation between build time and surface roughness in the grey relational grade, and the p-value was higher than 0.05 significant level. However, the surface roughness for optimal level combination setting showed the obvious result, which the settings consist of printing temperature (level 1), layer thickness (level 1), and surface layer (level 1).

Keywords: Ultrasonic vibration, surface roughness, Taguchi method, ANOVA, FDM

Abstrak

Artikel ini membentangkan parameter proses untuk pengoptimuman kekasaran permukaan specimen cetakan bagi pemodelan pemendapan tergabung (FDM) berbantukan getaran ultrasonik. Filamen *Acrylonitrile Butadiene Styrene* (ABS) telah dipilih sebagai bahan kajian. Suhu cetakan, ketebalan lapisan dan lapisan permukaan adalah parameter kawalan yang mempengaruhi kekasaran permukaan. Taguchi level 9 (3*3) *Orthogonal Arrays* (OA) telah digunakan didalam kajian ini dengan mengambil kira 9 kali data experimen. Terdapat 3 tahap di dalam setiap faktor kawalan yang telah dikenal pasti. Di samping itu, data pelbagai tindak balas untuk masa cetakan dan kekasaran permukaan, diperoleh dengan menggunakan dan menjalankan 9 kali eksperimen yang diperlukan didalam kaedah Taguchi. Specimen telah dihasilkan dengan 20kHz getaran ultrasonik yang disalurkan ke platform mesin FDM tersebut. Analisis varians (ANOVA) telah dijalankan untuk menentukan sama ada nilai-p adalah signifikan dengan model atau sebaliknya. Eksperimen ini telah mengkaji masa cetakan dan kekasaran permukaan, dan hasil tindak balas telahpun dikumpul dan dioptimumkan dengan menggunakan teknik *Gray Relational Grade (GRG)*. Hasil kajian menunjukkan tiada korelasi diantara masa cetakan dan kekasaran permukaan, dan nilai-p adalah lebih tinggi daripada nilai tahap ketara iaitu 0.05. Walau bagaimanapun, nilai kekasaran permukaan untuk gabungan

tahap yang digunakan didalam aras optimum telah menunjukkan hasil yang memberangsangkan, dimana kombinasi optimum terdiri daripada suhu cetakan (tahap 1), ketebalan lapisan (tahap 1), dan lapisan permukaan (tahap 1).

Kata kunci: getaran ultrasonik, kekasaran permukaan, kaedah Taguchi, ANOVA, FDM

1.0 INTRODUCTION

Additive manufacturing (AM) is a process that creates 3D object from CAD model by adding material layer by layer. AM has been continuously customized, redesigned and reimagined to a broad application in the industrial sector such as automotive, medical, architectural, aerospace, artistic and others [1]. AM gained the imagination of researchers and the public in various types of fields and obtained high popularity in media and brought revolution and improvement in the process of the product [2]. By using the layer-wise additive method, a complex shape can be built by using a wide variety of materials [3]. AM is different from conventional method as it perform by adding material and in contrast conventional manufacturing remove material to produce a part [4]. AM can boost creativity, production and service lead times cost-effectively while offering a high degree of manufacturing flexibility [5]. The implementation of low-risk, defect-tolerant modeling strategies is a guiding force for developing AM systems in real-world applications [6].

On the other hand, ultrasound has been widely used for machining, and it is a proven technology. A comparative study on traditional end-milling carbon fiber reinforced plastic with the one made with ultrasonic aided machining (UAM) [7] was done. The parameters of study are the surface integrity of the machined surface, cutting force and condition of the tool. In the ultrasonic machining, the piezoelectric ceramic material, such as barium titanate and the two metal electrodes constructed on the piezoelectric transducer's surface is employed. The pieces moved back and forth due to the alternating voltage from the wave generator to the electrodes on the piezoelectric transducer, causing the piezoelectric transducer to slightly vibrate. The transducer elements, which are the sonotrodes, vibrated at high frequencies and low amplitudes, causing mechanical vibration that can be utilized in machining processes [8]. After being compared with traditional machining, UAM showed a lower cutting force is required, better tool condition and better surface quality.

In addition, a study showed that using ultrasonic vibration in the AM process improves the surface finish of the FDM printed part [9]. A piezoelectric ultrasonic transducer was attached to the printer platform to apply the vibration while the printing process commences. Besides, the vibration frequency used was 11 kHz, 16 kHz, and 21 kHz. The surface roughness of the sample specimen printed was measured through the optical microscope. The finding indicates that ultrasonic aided printing can decrease surface roughness by 20% compared with standard test specimens. Furthermore, the finest surface finish was discovered when printing with 21kHz of ultrasonic vibration [9].

This article presents findings from the optimization of an open-source ultrasonic vibration assisted FDM process parameters for the best surface roughness of the printed ABS filament specimen using the Taguchi method. The surface roughness was investigated due to its affect on mechanical properties of the printed specimens such as dimensional accuracy , tesile or flextural strength. The control parameters that influenced the surface roughness determined are the printing temperature, layer thickness, and surface layer.

2.0 METHODOLOGY

2.1 Design of Experiment

As shown in Table 1, three control factors, namely, the printing temperature (°C), layer thickness (mm), and surface layer, were selected to examine the surface roughness of the ultrasonic vibration assisted FDM printing process. The three levels for each factor was established based on the literature review [10]. Table 2 shows the L_9 (3^3) Orthogonal Array (OA) with nine experimental runs included three control factors and two response values.

Table 1 Control factor of surface roughness and their levels

Control Factors	Unit	Levels		
		1	2	3
Printing Temperature	(°C)	240	250	260
Layer Thickness	(mm)	0.1	0.2	0.3
Surface Layer		3	4	5

Table 2. Experimental data gathering plan derived based on L_9 Taguchi Method

No. of Run	Control Factors			Response Value	
	Printing Temp. (°C)	Layer Thickness (mm)	Surface Layer	Build Time (min)	Surface Roughness, Ra (μ)
1	240	0.1	3	Q1	P1
2	240	0.2	4	Q2	P2
3	240	0.3	5	Q3	P3
4	250	0.1	4	Q4	P4
5	250	0.2	5	Q5	P5
6	250	0.3	3	Q6	P6
7	260	0.1	5	Q7	P7
8	260	0.2	3	Q8	P8
9	260	0.3	4	Q9	P9

$L_9 (3^3)$ Orthogonal Array

2.2 S/N Ratios in the Taguchi Method

To decrease the variance and optimize the process parameter, orthogonal arrays by Taguchi were employed. An evaluation of robustness is used in Taguchi designs to find control factors that decrease product or course changeability by restricting the repercussions of forwarding causes (noise factors), also known as S/N ratios [11]. The signal-to-noise ratio can be calculated by utilizing the noise called standard deviation and the proportion of signal commonly called mean. S/N ratios can measure the quality of the product. If the S/N ratios are higher, it means the quality of the desired parameter is high and should be more relatable with other parameters involved. The S/N ratio has three types of the desired improvement which are, higher-the-better, nominal-the-better and smaller-the-better, and their Equation (1) to (3) are shown below.

$$\left(\frac{S}{N}\right)_{h-t-b} = -10 * \log \left(\frac{1}{n}\sum_{i=1}^{n}\frac{1}{y^2}\right) \qquad (1)$$

$$\left(\frac{S}{N}\right)_{n-t-b} = -10 * \log \left(\frac{\bar{y}^2}{s^2}\right) \qquad (2)$$

$$\left(\frac{S}{N}\right)_{s-t-b} = -10 * \log \left(\frac{1}{n}\sum_{i=1}^{n}y_i^2\right) \qquad (3)$$

Where n- number of experiments, y_i– response value of the ith in the Orthogonal Arrays, $\bar{y}^2$- as mean and s^2- as the variance of the observed data.

2.3 Multi-Response Optimization Using Grey Relational Analysis (GRA)

GRA can be used to determine the response factor more than one for optimal response factor. Unreliable finite data can be optimized, and the GRA approach can generate a resemblance result. Additionally, Multi response of performance surface roughness is shown below with a complete step-by-step equation and

explanation [12]. In GRA, when the standard value and reference sequence range are considerably high, the function of the factors is neglected. When the standard value and reference sequence range are both so large, the factor will be ignored. When a factor has a nonidentical direction, GRA can produce nonsignificant results. The pre-processing data was created to determine the sequence from 0 to 1. This approach processed the data by sequence into the group, normalizing it in terms of grey relational generation, the two-quality characteristic of the important sequences, which are the larger-the-better or smaller-the-better [13]. For Equation (4), it can calculate the smaller-the-better and this suggested formula if the data desired must be less than the initial design parameter.

$$x_i^*(k) = \frac{maxy_i(k) - y_i(k)}{maxy_i(k) - miny_i(k)} \qquad (4)$$

2.3.1 Computation of Grey Relational Coefficient and Grade

The deviation sequence of the reference sequence will be calculated after the sequence data is standardized by using Equation (5):

$$\Delta_{0i}(k) = |x_0^*(k) - x_i^*(k)| \qquad (5)$$

Where $\Delta_{0i}(k)$ referred to the deviation, $x_0^*(k)$ referred to reference and $x_i^*(k)$ referred to comparability sequences. Then, to calculate the grey relational coefficient (GRC), Equation (6) was utilized.

$$\xi_i(k) = \frac{\Delta_{min}(k) - \zeta\Delta_{max}(k)}{\Delta_{0i}(k) - \zeta\Delta_{max}(k)} \qquad (6)$$

Grey relational coefficient, $\xi_i(k)$ were calculated and regularized as a function of Δ_{min} and Δ_{max} of every response, variable to determine whether the data value is minimum or the maximum deviations occur. The symbol of ζ represents the distinguishing coefficient, and it can also be called the identification coefficient, and it is circumscribed in the range of $\zeta \in [0,1]$, and usually, a value of ζ is 0.5. To determine the GRG, Equation (7) below can be computed.

$$\gamma_i = \frac{1}{n}\sum_{i=1}^{n}\xi_i \qquad (7)$$

Where γ_i represent the value of GRG, ith for the experimental and n= number of responses. After the optimal level is discovered, the last step is to predict and prove the quality characteristics by using Equation (8). The good experiment value is higher than the predicted value and their initial design value.

$$\gamma_{predicted} = \gamma_m \sum_{i=1}^{nq} \gamma_o - \gamma_m \qquad (8)$$

Where γ_m indicates the mean of grey relational grade and γ_o indicates the maximum average of grey relational grade. Finally, response values affected by q are denoted as the number of factors in the analysis of GRG.

2.4 Analysis of Variance (ANOVA)

The response accuracy prediction using ANOVA modeling to determine the correlation between parameters through a mathematical approach can be demonstrated [14]. Using ANOVA on the identified design, a significant effect on the response can be evaluated. If the value of Prob > F, often known as a p-value, is less than 0.05, the model is significant [15]. Adjusted correlation coefficient R^2_{adj} is used to analyze the model effectiveness. On the whole, R^2 and R^2_{adj} should be higher and comparable with each other to ensure the optimal design parameter is more reliable to the model of analysis [16].

2.5 Experimental Set-Up

Acrylonitrile butadiene styrene (ABS) material was used in this experiment as it is a common material used in AM. Table 3 shows the mechanical properties of the ABS.

Table 3 Properties of ABS; Source [17]

Property	ABS
Printing temperature (°C)	210-250
Build platform temperature (°C)	80 -110
Raft	Mandatory
Strength	Medium
Flexibility	Moderately flexible
Heat Resistance	Moderate
Biodegradability	No
Moisture absorption	Yes

The test specimen was designed using CAD software and then transfered to STL file format then was feed to the FDM printer (UP Plus 2). Specimens were designed rectangle with height, width, and thickness of 80 mm, 30 mm, and 5 mm, respectively, as shown in Figure 1. The printer with the piezoelectric transducer mounted on the build platform as shown in Figure 2. The transducer was supplied with a fixed signal of 20kHz sine-waveform, to generate the ultrasonic vibration during the printing process as shown in Figure 3. Before the printing process began, the printer's parameter was set according to the desired experimental result. Printing speed was set to 'NORMAL' in the software UP Studio which indicated $50 cm^3/h$. As illustrated in Figure 4 (experimental set up)

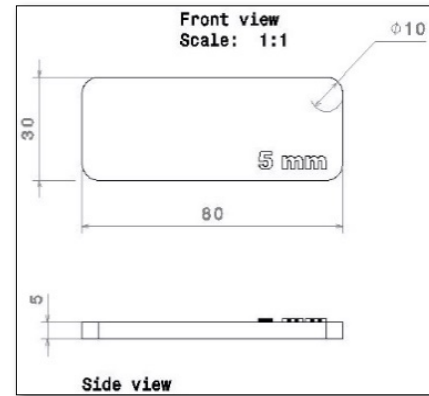the specimens were printed according to the combination level in the Taguchi Orthogonal Arrays.
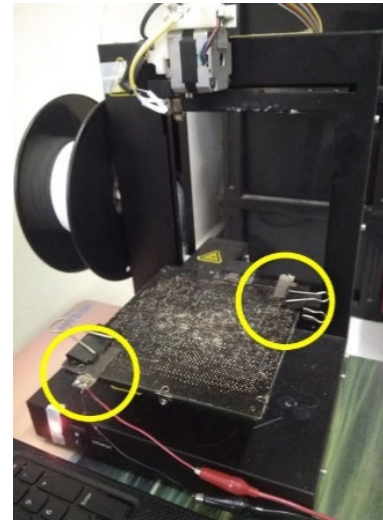

Figure 1 Specimen Dimensions

Figure 2 Ultrasound transducer placed on both sides of the build platform
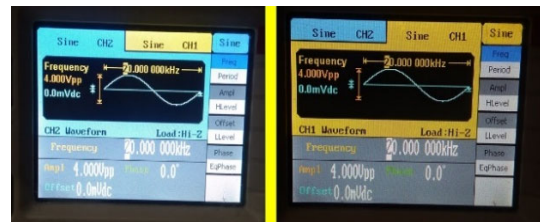

Figure 3 Sine-wave was set to 20KHz frequency for both output channel 1 (CH1) and channel 2 (CH2)

Figure 4 Ultrasound-assisted FDM experimental setup

To conduct a surface roughness test, a touch probe of Mitutoyo Suftest SJ-301 was used to measure the surface roughness. The machine was set, and the area of surface roughness experiment was determined. The probe was put on the specimens as shown in Figure 5 and surface roughness was measured several times to gather reliable value of surface roughness, and the average value was calculated on each printed specimen. After all surface roughness value was collected, the next step was to perform the microscopic inspection using the Meiji Stereo Microscope. Figure 6 displays the specimens that were placed on the microscope and the image was recorded. The desired images were then captured using tools or software that come with the microscope machine itself. Images containing the surface inspection were utilized and studied whether there are defects on the surface or otherwise. The data gathered was then concluded to determine which combination of parameters was the most significant in determining the good surface finish of the test specimen.
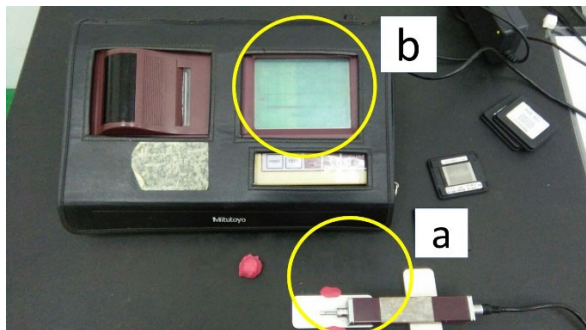

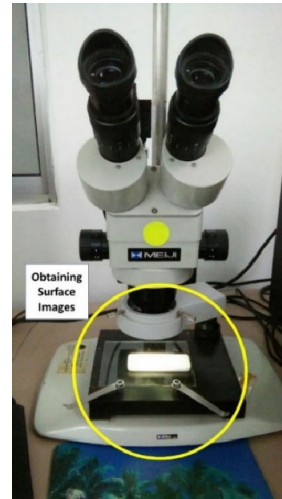**Figure 5** Mitutoyo Suftest SJ-301 to measure the surface roughness

Figure 6 Meiji Stereo Microscope used to analyze the surface of printed specimens

3.0 RESULT AND DISCUSSION

Table 4 were transformed to S/N ratios to investigate Taguchi's L_9 Orthogonal Arrays using Grey Relational Analysis. In this study, response value of build time and surface roughness was investigated with the affect of the control factors namely the printing temperature, layer thickness, and surface layer. The affect of factors on multiple responses was examined using attributes of aspect smaller-the-better, as build time and surface roughness lower values were desired.

Table 4 Taguchi L_9 Orthogonal Array and multi-response results with signal to noise (S/N) Ratio

Run	Printing Temperature (°C)	Layer Height (mm)	Surface Layer	Build Time (min)	Surface Roughness, Ra (μm)	Built Time
1	240	0.1	3	85	0.644	-38.5884
2	240	0.2	4	42	2.348	-32.465
3	240	0.3	5	29	2.284	-29.248
4	250	0.1	4	84	1.156	-38.4856
5	250	0.2	5	45	2.004	-33.0643
6	250	0.3	3	25	3.046	-27.9588
7	260	0.1	5	86	2.076	-38.69
8	260	0.2	3	39	3.084	-31.8213
9	260	0.3	4	27	3.204	-28.6273

3.1 Effect of the Control Factors on Build time

The experiment data of build time in Table 4 were converted into S/N ratios using Minitab@19 statistical software. Delta statistics in the response table for S/N ratios as shown in Table 5 below represent the leading control factors. The highest and the lowest of each factor were calculated to produce the delta statistics. The value delta which is the highest was assigned the first in the rank and represents the leader of the factor that affects build time. The most significant factor in Table 5 is the layer thickness with the delta value of

9.98. The surface layer is the second most influential factor with the delta value of 0.88, followed by the printing temperature of 0.39.

Table 5 Response table for S/N ratios of build time (min)

Level	Printing Temperature (°C)	Layer Thickness (mm)	Surface Layer
1	-33.43	-38.59	-32.79^1
2	-33.17	-32.45	-33.19
3	-33.05^1	-33.05^1	-33.67
Delta	0.39	9.98	0.88
Rank	3	1	2

[1] Desired factor levels

From the response in Table 5, the main effects plot for S/N ratios was generated as illustrated in Figure 7. Build time is strongly impacted by variations in the layer thickness as indicated in the trend of the plot. As can be translated from Table 5, the build time is decreased when the layer thickness is increased. The observation of the aspect of the response is enhanced when the layer thickness increase, this is strengthened by increasing the trend of S/N ratios for build time from 0.1 mm to 0.3 mm in the layer thickness. The printing temperature shows a slight increase in the S/N ratio trend from 240 °C to 260 °C. The S/N showed a slightly decreased trend for the surface layer which was from 3 layers to the 5 layers. The primary effect plot for S/N ratios in Figure 7 recommends that Printing Temperature (Level 3), Layer Thickness (Level 3) and Surface Layer (Level 1) are the desired factor levels to obtain high S/N ratios and lower values of build time (min).
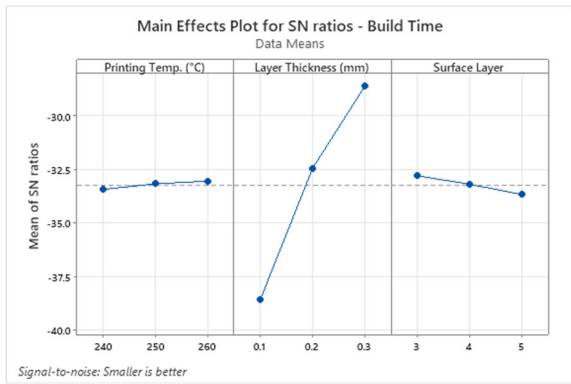

Figure 7 Main effect plot for S/N Ratios of Build time

After that, to determine the factor levels, Table 6 shows an ANOVA was performed to gather each factor of percentage contribution that affect the build time. Layer thickness with a contribution of 98.94 %, has the highest dominance on the build time followed by surface layer, with a contribution of 0.76 %, and then printing temperature with 0.15 % of the contribution. At a 95% confidence level, factors having a p-value less than 0.05 are considered

significant [18]. The change in the build time was significantly contributed by the $p-values$ of layer thickness which is less than 0.05. Also, it can be seen from the Table 6 that are high and comparable values R^2 and R^2_{adj} with each other. This is signed the rightness served of the model [19].

Table 6 ANOVA for S/N ratio of build time (min)

Source	DF	Adj SS	Adj MS	F	F	Contribution (%)	Remarks
Printing Temperature	2	2.67	1.33	0.57	0.636	0.05	Not significant
Layer Thickness	2	5438	2719	1165.29	0.001	99.49	Significant
Surface Layer	2	20.67	10.33	4.43	0.184	0.38	Not significant
Error	2	4.67	2.33			0.09	
Total	8	5466		S = 1.52753		$R^2 = 99.91\%$	$R^2_{adj} = 99.66\%$

3.3 Confirmation Test for Build Time (min)

To abolish the disturbance about the preferred control factors, acceptance of responses, and experimental design, the tool is commonly used as a confirmation test from the parameter design by the Taguchi method as mentioned in the previous study by [20]. Once the optimal setting has been identified, the next step is trying to predict and verify the performance improvement of the responses whether there are some improvement products from the experiment value. The good in confirmation experiment result with the prediction value is shown in Table 7. The predicted S/N ratio was calculated using Equation (3) which considers smaller the better for the value. It can be decoded from Table 7, the optimal process parameters for the experiment value, the percentage reduction of build time shown an improvement of 13.79% which is comparable with the prediction value of 14.93%. In terms of the improvement in the S/N ratio, there are some increases in the experiment value by 1.2892 from the initial design parameters of the S/N ratio value and also proportionate with the value of prediction of improvement in S/N ratio of 1.4046 points. This improvement in the experimental result over the initial design parameter guaranteed the effectiveness of the S/N ratio analysis from the Taguchi method for ultrasonic vibration-assisted FDM.

Table 7 Results of the confirmation experiment Build time

Initial process parameter		Optimal process parameters	
		Prediction	Experiment
Setting level	PT(1) – LT(1) – SL(3)	PT(3) – LT(3) – SL(1)	PT(3) – LT(3) – SL(1)
Surface roughness, Ra (μm)	29	24.67	25
S/N ratio (dB)	-29.248	-27.8434	-27.9588
Improvement in S/N ratio (dB)		1.4046	1.2892
Percentage reduction of surface roughness		14.93%	13.79%

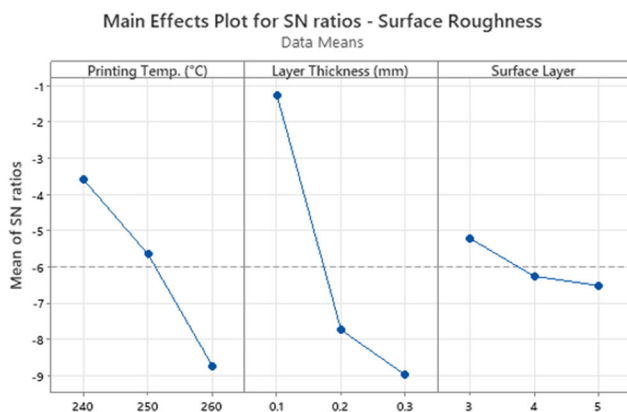## 3.2 Effect of the Control Factors on Surface Roughness, Ra (μm)

To determine the factors influencing the surface roughness, the S/N ratios of the experimental data of Ra were calculated as shown in Table 8. Similar to build time analysis, smaller-the-better characteristic of the Taguchi method was selected to investigate factor effects. The response table for the S/N ratios of Ra was then generated, as shown in Table 8. The results indicate that the layer thickness, with a delta of 7.727, has the highest effect on Ra, followed by printing temperature and surface layer, with deltas of 5.158 and 1.307, respectively.

Table 8 Response table for S/N ratios of Surface Roughness, Ra (μm)

Level	Printing Temperature (°C)	Layer Thickness (mm)	Surface Layer
1	-3.589 [1]	-1.260 [1]	-5.212 [1]
2	-5.657	-7.745	-6.262
3	-8.747	-8.987	-6.519
Delta	5.158	7.727	1.307
Rank	2	1	3

[1] Desired factor levels

As illustrated in Figure 8, the response table for S/N ratios was then used to obtain the plot of primary effects for surface roughness. Ratio decreases with an increase in the printing temperature and layer thickness can be analyzed. In the case of the surface layer, there is a slight decrease in the ratio between 3 to 5 layers. Figure 8 shows that the desirable values of S/N of surface roughness are achieved at the first level of Printing temperature (Level 1), the first level of layer thickness (Level 1), and the first level of the surface layer (Level 1). Besides, printing temperature mainly affects the delta statistics, followed by layer thickness and surface layer.

Figure 8 Main effect plot for S/N Ratios of Surface Roughness

Subsequently, ANOVA was performed in Table 9 below and studied to determine the significant factors and the percentage of contribution of each factor to the response of surface roughness. Layer thickness has the highest percentage contribution of 45.72%, followed by printing temperature of 33.62% and surface layer 20.54%. Further, p-values of each factor that contribute to surface roughness are all less than 0.05. The experiment's outcome p-values less than 0.05 offered strong evidence that the data obtained solidly supported the null hypothesis [21]. It can be concluded that all the parameters are essential to determine the surface roughness performance of ultrasonic vibration assisted FDM. The high and comparable R^2 = 99.88% with R^2_{adj} = 99.51%, affirms that the model is good and valid.

Table 9 ANOVA for S/N ratio of Surface Roughness, Ra (μm)

Source	DF	Adj SS	Adj MS	F	F	Contribution (%)	Remarks
Printing Temperature	2	7.5751	3.78755	273.11	0.004	33.62	Significant
Layer Thickness	2	10.3021	5.15103	371.42	0.003	45.72	Significant
Surface Layer	2	4.6274	2.31372	166.84	0.006	20.54	Significant
Error	2	0.0277	0.01287			0.12	
Total	8	5466		S = 0.117764		R^2 = 99.99%	R^2_{adj} = 99.51%

3.3 Confirmation Test for Surface Roughness, Ra

Table 10 shows the confirmation experiment surface roughness after the initial process parameter has been identified. Since the deltas of S/N ratios ranked and agreed with the previous initial experiment, the value of surface roughness is the same, which is 0.644 μm, and there is no need to run the new investigation. The result for the confirmation experiment with the prediction value desire has complied with each other, and it presented the goodness of the analysis model. The experiment value shows some reduction from the initial design parameter of 2.284 μm reduce to 0.644 μm, and the prediction value also admits it of 0.898 μm for 'Setting Level' of the printing time (level 1), layer thickness (level 1), and surface layer (level 1). This result proves by the improvement in the S/N ratio by 3.351 points and higher than the initial design parameter and prediction value which are -7.1739 and 0.9345, respectively. Percentage reduction of surface roughness value of 71.8 % is comparable with the prediction value of 60.68 %. It is also representing the good of the model used in this analysis.

Table 10 Results of the confirmation experiment surface roughness, Ra

Initial process parameter		Optimal process parameters	
		Prediction	Experiment
Setting level	PT(1) – LT(1) – SL(3)	PT(3) – LT(3) – SL(1)	PT(3) – LT(3) – SL(1)
Surface roughness, Ra (μm)	2.284	0.898	0.644
S/N ratio (dB)	-7.1739	0.9345	3.8223
Improvement in S/N ratio (dB)		6.2394	3.351
Percentage reduction of surface roughness		60.68%	71.80%

3.3   Confirmation Test of GRG

Even though the null hypothesis is accepted, the result have to be confirmed in case the p-value produce the wrong value, because some of the experiment produces the wrong p-value and resulting in the wrong discussion [22]. The predicted GRG was calculated using Equation (8). The grey relational grade (GRG) was calculated and averaged from the three runs. The optimized level has been determined from the response GRG Table 11 and the new result for build time and surface roughness were 24 (min) and 2.182 (μm), respectively.

Further, it can be inferred from Table 11 that the result of the experiment value prove that the null hypothesis was correct because the value gathered does not exceed the initial design value and decreased the value of grey relational analysis to (-10.77%) even though the prediction value says it will increase the grey relational value by 13.45%. This result affirms that the p-value state that the result of the experiment will not be relatable with each of the response parameters, and it is proved p-values less than 0.05 only provide a significant result [23].

Table 11 Results of the experiment

Initial Design Parameters		Optimal Design Parameters	
		Prediction	Experiment
Setting Level	PT (1)-LT (3)-SL (3)	PT (1)-LT (3)-SL (1)	PT (1)-LT (3)-SL (1)
Grey relational grade	0.6612	0.750124	0.589881
Improvement in GRG		13.45%	-10.77%

*PT-printing temperature, LT-layer thickness, SL-surface layer

3.4   Macroscopic Inspection

Macroscopic inspection for optimal surface roughness was done. The specimens printed were examined by macroscopic inspection using the Meiji Stereo Microscope to find the structure difference on the specimen, as shown in Figure 9. To examine the printed sample surface, the magnification of 1.5X to 420X and accuracy of 0.05 mm are set accordingly. This stereo microscope is connected with a digital camera and personal computer as it is used to capture the visual of the sample surface and display it. There is no evidence of gaping and air bubbles trapped in between the layer of the printed specimen. The surface of the specimen has a small and fine gap between extruded material of 0.1 mm layer thickness, then created smooth surface roughness, which is an average of 0.644 μm.
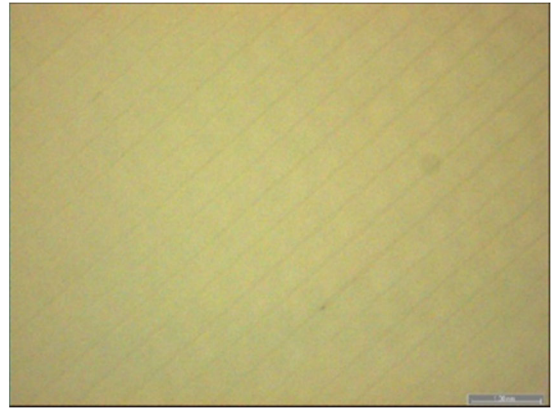

Figure 9 Printed specimen by optimal surface roughness setting level of printing speed (level 1), layer thickness (level 1), and surface layer (level 1)

3.5   Macroscopic Inspection for Optimal Grey Relational Grade (GRG)

Macroscopic inspection for the optimal grey relational grade was examined by determining the changes in the surface roughness of printed specimen with optimized level, as shown in Figure 10. However, the surface roughness for this printed specimen is not very smooth, and the value of surface roughness, Ra is 2.182 μm. The wavy and big gap created by the extruded material of layer thickness of 0.3 mm is unlike that already described in the optimal surface roughness section. Figure 10 also indicates no evidence of crack or bubble on the specimen and concludes this specimen is still reliable. Nonetheless, in terms of build time, regardless of surface roughness, the specimen printed in optimal GRG has an excellent build time of 25 min was one of the lowest build times in the experiment.

Figure 10 Printed specimen by optimal grey relational grade (GRG) setting level of printing speed (level 1), layer thickness (level 3), and surface layer (level 1)

4.0 CONCLUSION

This paper aims to optimize the parameter of an open-source ultrasonic vibration assisted FDM printer for surface roughness. Initially, the outcome of control factors which are printing temperature, layer thickness, and surface layer on the GRG, does not meet the desired value, which means there is no relatable surface roughness and build time. This is also proven by the p-values that indicated higher than 0.05 of significant level. The parameter for surface roughness was then optimized by using ANOVA on signal-to-noise ratios (S/N ratios). The value of surface roughness was 0.644µm, which shows that the surface of the specimen was very smooth, and the gap between extruded material hardly appears. There is also no crack or bubble present. To conclude, the ANOVA model did improve the surface roughness of the printed specimen, and the setting level of printing temperature (level 1), layer thickness (level 1), and surface layer (level 1) has revealed to be the most optimal control response in the model experiment.

Acknowledgement

References

[1]   Sheridan, L., J. E. Gockel, and O. E. Scott-Emuakpor. 2021. Stress-defect-life Interactions of Fatigued Additively Manufactured Alloy 718. *Int. J. Fatigue*. 143(August): 106033.

[2]   Zhu, J., H. Zhou, C. Wang, and L. Zhou. 2020. A Review of Topology Optimization for Additive Manufacturing: Status and Challenges. *Chinese J. Aeronaut.* October: 20.

[3]   Marmarelis, M. G.and R. G. Ghanem. 2020. Data-driven Stochastic Optimization on Manifolds for Additive Manufacturing. *Comput. Mater. Sci*. 181(March): 109750.

[4]   Yadav, D. K., R. Srivastava, and S. Dev. 2019. Design & Fabrication of ABS Part by FDM for Automobile Application. *Mater. Today Proc*. 26: 2089-2093.

[5]   Daminabo, S. C., S. Goel, S. A. Grammatikos, H. Y. Nezhad, and V. K. Thakur. 2020. Fused Deposition Modeling-based Additive Manufacturing (3D printing): Techniques for Polymer Material Systems. *Mater. Today Chem*. 16: 100248.

[6]   Eswaran, P., K. Sivakumar, and M. Subramaniyan. 2018. Minimizing Error on Circularity of FDM Manufactured Part. *Mater. Today Proc*. 5(2): 6675-6683.

[7]   Huda, A. H. N. F., H. Ascroft, and S. Barnes. 2016. Machinability Study of Ultrasonic Assisted Machining (UAM) of Carbon Fibre Reinforced Plastic (CFRP) with Multifaceted Tool. *Procedia CIRP*. 46: 488-491.

[8]   Yang, C. H., N. Jeyaprakash, and C. K. Chan. 2020. Inhomogeneous Mechanical Properties in Additively Manufactured Parts Characterized by Nondestructive Laser Ultrasound Technique. *NDT E Int*. 116(August): 102340.

[9]   Maidin, S., M. K. Muhamad, and E. Pei. 2015. Feasibility Study of Ultrasonic Frequency Application on FDM to Improve Parts Surface Finish. *J. Teknol.* 77(32): 27-35.

[10] Panda, A., A. K. Sahoo, and A. K. Rout. 2016. Multi-attribute Decision Making Parametric Optimization and Modeling in Hard Turning using Ceramic Insert through Grey Relational Analysis: A Case Study. *Decis. Sci. Lett*. 5(4): 581-592.

[11] Rajendra B., and D. Deepak. 2016. Optimization of Process Parameters for Increasing Material Removal Rate for Turning Al6061 Using S/N Ratio. *Procedia Technol*. 24: 399-405.

[12] Meel R., V. Singh, P. Katyal, and M. Gupta. 2021. Optimization of Process Parameters of Micro-EDD/EDM for Magnesium Alloy using Taguchi based GRA and TOPSIS Method. *Mater. Today Proc*. 2: 1-7.

[13] Singh G., S. Singh, D. Parkash, V. Gulati, and T. Kaur. 2018. Optimization of EN24 Steel on EDM Machine using Taguchi & ANOVA Technique. *Mater. Today Proc*. 5(14): 27974-27981.

[14] Chakrapani P.and T. S. A. Suryakumari. 2021. Modelling and Analysing the Water Jet Machining Parameters of Aluminium Nano Composite by ANOVA and Taguchi. *Mater. Today Proc*. 3.

[15] Marini F., and B. Walczak. 2020. *ANOVA-Target Projection (ANOVA-TP)*. 2nd ed. Elsevier Inc.

[16] Vishwanatha J. S., A. M. Hebbale, N. Kumar, M. S. Srinath, and R. I. Badiger. 2021. ANOVA Studies and Control Factors Effect Analysis of Cobalt Based Microwave Clad. *Mater. Today Proc*. 46: 2409-2413.

[17] A. Dey and N. Yodo. 2019. A Systematic Survey of FDM Process Parameter Optimization and Their Influence on Part Characteristics. *J. Manuf. Mater. Process*. 3(3).

[18] Griffiths P. and J. Needleman. 2019. Statistical Significance Testing and p-values: Defending the Indefensible? A Discussion Paper And Position Statement. *Int. J. Nurs. Stud*. 99: 1-5.

[19] Mohsin I., K. He, Z. Li, F. Zhang, and R. Du. 2020. Optimization of the Polishing Efficiency and Torque by using Taguchi Method and ANOVA in Robotic Polishing. *Appl. Sci*. 10(3).

[20] Kim N. P., D. Cho, and M. Zielewski. 2019. Optimization of 3D Printing Parameters of Screw Type Extrusion (STE) for Ceramics using the Taguchi Method. *Ceram. Int*. 45(2): 2351-2360.

[21] Chen X., and S. K. Sarkar. 2020. On Benjamini–Hochberg Procedure Applied to Mid p-values. *J. Stat. Plan. Inference*. 205: 34-45.

[22] Garamszegi L. Z., and P. De Villemereuil. 2017. Perturbations on the Uniform Distribution of p-values Can Lead to Misleading Inferences from Null-hypothesis Testing. *Trends Neurosci. Educ*. 8-9(July): 18-27.

[23] Sylajakumari P. A., R. Ramakrishnasamy, and G. Palaniappan. 2018. Taguchi Grey Relational Analysis for Multi-response Optimization of Wear in Co-continuous Composite. *Materials (Basel)*. 11(9): 1-17.